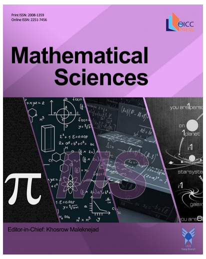

Math. Sci. 2025; 19(3): 1-14

Mathematical Sciences (MS)

https://doi.org/10.57647/mathsci.2025.1903.15

Numerical Computation of Solutions and Truncation Error for Stochastic Differential Equations of Order 1.5

Yazid Alhojilan*

Department of Mathematics, College of Science, Qassim University, Saudi Arabia

***Corresponding author:** yhjielan@qu.edu.sa

Original Research

Received:
10 August 2025

Revised:
26 August 2025

Accepted:
3 September 2025

Published in Issue:
30 September 2025

Abstract:

A recent study proposed a groundbreaking pathwise approximation method for numerically solving stochastic differential equations (SDEs) driven by Brownian motions. This approach eliminates the necessity of simulating stochastic Itô integrals, denoted by $\mathcal{J}_\alpha$. Instead, these integrals are replaced with random variables that maintain the same moments under the linear term condition. The main objective of this method is to deliver approximate solutions with an error rate of $O(h^{\frac{3}{2}})$. This level of precision significantly exceeds the strong error rates achieved by the Euler and Milstein methods, which are $O(\sqrt{h})$ and $O(h)$, respectively, where h represents the step size. The development of this method relies on the assumption that the diffusion process is nondegenerate and incorporates the Itô-Taylor expansion alongside a modified perturbation approach. In this paper, we demonstrate that the scheme achieves strong convergence in the Wasserstein distance with an order of $O(h^{\frac{3}{2}})$ by leveraging techniques from the optimal transport theory.

Keywords: Stochastic Differential Equations; Stochastic Systems; Strong Convergence; Itô–Taylor Expansion; Coupling Method; High-Order Numerical Scheme; Numerical Results

Cite this article: Alhojilan Y. Numerical Computation of Solutions and Truncation Error for Stochastic Differential Equations of Order 1.5. Math. Sci 2025; *19*(3): 1-14 https://doi.org/10.57647/mathsci.2025.1903.13

1. Introduction

Stochastic differential equations (SDEs) have extensive applications in fields such as biology, finance, engineering, chemistry, mechanics, and economics. They are crucial in modeling real-world systems affected by randomness or uncertainty. However, exact analytical solutions are rarely available in practice. This limitation motivates the development of accurate and computationally efficient numerical methods for SDEs, which can provide reliable approximations of system behavior under random influences. The main goal of this study is to introduce an approach that overcomes the high computational cost and complexity of traditional schemes, particularly for higher-dimensional problems. In cases where explicit solutions to these equations are not available, numerical methods must be developed to obtain approximate solutions. Most of the commonly used methods for approximating SDEs, such as the Euler and Milstein methods, are based on Itô–Taylor or Stratonovich–Taylor expansions and offer solution accuracies of order $\frac{1}{2}$ and 1, respectively. To achieve higher-order approximations, additional terms from these expansions are typically included. However, this approach poses significant challenges, particularly when calculating iterated stochastic integrals $\mathcal{J}_\alpha$, especially in the case of high-dimensional Brownian motion (dimensions greater than two). Several methods have been proposed to address these challenges and provide higher-order approximations, as seen in works such as [1, 2, 3, 4, 5, 6, 7, 8, 9, 10, 11, 12, 13]. However, these methods often fail to achieve the desired efficiency due to computational complexity or limitations in extending to higher dimensions. For example, the method presented in [10] for generating double stochastic integrals $\mathcal{J}_\alpha$ is sufficient for first-order approximations but cannot be easily extended to more than two dimensions due to its computational burden. Similarly, while Kloeden and Platen [11] developed a method based on Fourier series to approximate SDEs, their approach encounters difficulties in computing iterated stochastic integrals when the dimension exceeds two. These considerations motivate the present work, which introduces a novel scheme specifically designed to overcome the outlined limitations by streamlining the computation and improving efficiency, especially for high-dimensional problems.

The proposed numerical scheme achieves a strong convergence order of $O(h^{3/2})$. Its main advantage lies in replacing the stochastic integrals $\mathcal{J}_\alpha$ by suitably constructed random variables that share identical moments with respect to the dominant linear term. This eliminates the need for the direct computation of iterated stochastic integrals, thereby significantly simplifying the implementation and enhancing computational efficiency. The method reformulates the stochastic expansion as a perturbation of the linear component, following the approach introduced by Davie [14, 15, 16] and further applies a coupling technique from optimal transport theory to obtain a high-quality mean-square approximation. As a result, higher-order accuracy is achieved at a substantially reduced computational cost, even in high-dimensional settings. The scheme is readily extendable to broader classes of stochastic differential equations and has been validated through extensive numerical experiments assessing both strong errors and weak truncation errors. However, the theoretical guarantees are strongest in the case of non-degenerate diffusion matrices; in degenerate or singular settings, additional modifications may be required for optimal performance, which remains an interesting direction for future research.

Recent progress in the numerical solution of stochastic and fractional integro-differential equations has produced powerful frameworks based on polynomial, barycentric, meshless, and spectral interpolation techniques. Notable examples include the Vieta–Lucas polynomial technique for nonlinear stochastic Itô–Volterra integral equations [17]; meshless barycentric rational interpolation methods for nonlinear stochastic fractional integro-differential equations [18]; enhanced moving least squares techniques for Hammerstein-type stochastic fractional Volterra integro-differential equations [19]; Floater–Hormann interpolation for accurate and stable computation in stochastic Itô–Volterra integral equations [20]; and spectral methods based on Mittag-Leffler wavelets for stochastic differential equations [21]. In addition, several recent studies by Badawi and collaborators have made significant theoretical and numerical contributions to stochastic fractional modeling. These include the analysis of stochastic M-fractional differential models using matrix spectral collocation techniques [22]; the development of step spectral collocation methods for stochastic fractional systems with constant delays [23]; the introduction of shifted Legendre spectral schemes for Hilfer-type stochastic integro-differential equations [24]; and the proposal of a shifted Legendre–Gauss pseudospectral algorithm for fractional M-derivative stochastic models [25]. The integration of these advanced fractional and spectral approaches with coupling-based stochastic schemes, as proposed here, highlights the growing scope of high-order stochastic solvers and provides context for the contributions of the present work.

Finally, we highlight the role of pathwise approximation, which ensures that the numerical method accurately captures individual sample trajectories, not only expectations. Within the Itô–Taylor expansion framework, the substitution of higher-order stochastic integrals by random variables with matching statistical moments allows the scheme to retain the strong convergence order $O(h^{3/2})$ while avoiding explicit computation of iterated integrals. The paper is organized as follows. Section 2 presents the necessary background material, Section 3 describes the numerical methodology and computation of the solutions, Section 4 focuses on the analysis of the truncation error, and the final section contains concluding remarks.

2. Background

Consider a probability space $(\Omega, \mathcal{F}, \mathbb{P})$ equipped with a filtration $\mathcal{F} = (\mathcal{F}_t)_{t\geq 0}$, and let $Z_t = (Z_t^1, \ldots, Z_t^M)_{t\geq 0}$ be an M-dimensional Brownian motion adapted to $\mathcal{F}$. A general q-dimensional Itô stochastic differential equation (SDE) is given by:

$$d\hat{y}_t = c(t, \hat{y}_t)\, dt + \sum_{k=1}^{M} \sigma_k(t, \hat{y}_t)\, dZ_t^k$$
$$\hat{y}_0 = \hat{y}^{(0)} \qquad 0 \leq t \leq T. \tag{1}$$

Here, $\hat{y}_t \in \mathbb{R}^q$ denotes the exact continuous-time solution of the stochastic differential equation. The coefficient functions $c(t, \hat{y}) : \mathbb{R}^q \to \mathbb{R}^q$ and $\sigma_k(t, \hat{y}) : \mathbb{R}^q \to \mathbb{R}^q$ are assumed to be Borel measurable, and the process $\hat{y}_t$ is adapted to the filtration $\mathcal{F}_t$. In order to distinguish the analytical solution from its numerical approximation introduced in Section 3, we use the notation $\hat{y}^{(j)}$ to denote the discrete-time approximation at time $t_j = jh$.

The exact solution satisfies the following integral equation:

$$\hat{y}_t = \hat{y}_0 + \int_0^t c(s, \hat{y}_s)\, ds + \sum_{k=1}^{M} \int_0^t \sigma_k(s, \hat{y}_s)\, dZ_s^k \tag{2}$$

where the stochastic integrals are understood in the Itô sense.

2.1 Itô–Taylor Expansion

A powerful method for analyzing and numerically approximating SDEs is the Itô–Taylor expansion, which generalizes the classical Taylor series to stochastic processes. For a scalar SDE,

$$\hat{y}_t = \hat{y}_0 + \int_{t_0}^t c(s, \hat{y}_s)\, ds + \int_{t_0}^t \sigma(s, \hat{y}_s)\, dZ_s \qquad t \in [t_0, T], \tag{3}$$

The Itô formula applies to functions $f : \mathbb{R} \to \mathbb{R}$ that are twice continuously differentiable:

$$f(\hat{y}_t) = f(\hat{y}_0) + \int_{t_0}^t \Big[c(s, \hat{y}_s) \frac{\partial f(\hat{y}_s)}{\partial \hat{y}} + \frac{1}{2}\sigma^2(s, \hat{y}_s) \frac{\partial^2 f(\hat{y}_s)}{\partial \hat{y}^2} \Big] ds + \int_{t_0}^t \sigma(s, \hat{y}_s) \frac{\partial f(\hat{y}_s)}{\partial \hat{y}}\, dZ_s \tag{4}$$

https://doi.org/10.57647/mathsci.2025.1903.15

or, equivalently,

$$f(\hat{y}_t) = f(\hat{y}_0) + \int_{t_0}^{t} L^0 f(\hat{y}_s)\, ds + \int_{t_0}^{t} L^1 f(\hat{y}_s)\, dZ_s \tag{5}$$

where the differential operators are given by:

$$L^0 = c\frac{\partial}{\partial \hat{y}} + \frac{1}{2}\sigma^2 \frac{\partial^2}{\partial \hat{y}^2} \qquad L^1 = \sigma \frac{\partial}{\partial \hat{y}} \tag{6}$$

Setting $f(\hat{y}) = \hat{y}$ recovers the original SDE, while $f = c$ or $f = \sigma$ produces higher-order stochastic terms. The development proceeds as follows:

$$\begin{aligned}
\hat{y}_t = \hat{y}_0 &+ \int_{t_0}^{t} \left[c(\hat{y}_0) + \int_{t_0}^{s} L^0 c(\hat{y}_z)\, dz \right. \\
&\left. + \int_{t_0}^{s} L^1 c(\hat{y}_z)\, dZ_z \right] ds \\
&+ \int_{t_0}^{t} \left[\sigma(\hat{y}_0) + \int_{t_0}^{s} L^0 \sigma(\hat{y}_z)\, dz \right. \\
&\left. + \int_{t_0}^{s} L^1 \sigma(\hat{y}_z)\, dZ_z \right] dZ_s
\end{aligned} \tag{7}$$

which can be expressed compactly as:

$$\hat{y}_t = \hat{y}_0 + c(\hat{y}_0) \int_{t_0}^{t} ds + \sigma(\hat{y}_0) \int_{t_0}^{t} dZ_s + R \tag{8}$$

with remainder term R given by nested integrals over L^0 and L^1.

2.2 Pathwise Approximation of SDEs Using Stochastic Taylor Expansions

Consider again the Itô SDE given by equation (1). For each component $i = 1, \dots, q$, the dynamics are described as:

$$(d\hat{y}_t)_i = c_i(t, \hat{y}_t)\, dt + \sum_{k=1}^{M} \sigma_{ik}(t, \hat{y}_t)\, dZ_t^k \quad (\hat{y}_0)_i = \hat{y}_i^{(0)} \tag{9}$$

where $\hat{y}_t \in \mathbb{R}^q$ denotes the state vector, and $Z_t \in \mathbb{R}^M$ represents an M-dimensional Brownian motion.

We assume that this SDE satisfies the standard conditions ensuring the existence and uniqueness of solutions. To approximate the solutions pathwise, the interval $[0, T]$ is divided into N subintervals of equal length $h = \frac{T}{N}$. In each subinterval, stochastic Taylor expansions provide accurate approximations to the solution trajectories.

The classical Euler–Maruyama scheme approximates the dynamics by:

$$\hat{y}_i^{(j+1)} = \hat{y}_i^{(j)} + c_i(jh, \hat{y}^{(j)})h + \sum_{k=1}^{M} \sigma_{ik}(jh, \hat{y}^{(j)}) \Delta Z_k^{(j)} \tag{10}$$

where $\Delta Z_k^{(j)} = Z_k((j+1)h) - Z_k(jh)$ are Brownian increments.

To achieve higher-order accuracy, the Milstein scheme incorporates quadratic terms:

$$\begin{aligned}
\hat{y}_i^{(j+1)} = \hat{y}_i^{(j)} &+ c_i(jh, \hat{y}^{(j)})h + \sum_{k=1}^{M} \sigma_{ik}(jh, \hat{y}^{(j)}) \Delta Z_k^{(j)} \\
&+ \sum_{k,l=1}^{M} \rho_{ikl}(jh, \hat{y}^{(j)}) \mathcal{J}_{kl}^{(j)}
\end{aligned} \tag{11}$$

where

$$\rho_{ikl}(t, \hat{y}) = \sum_{m=1}^{q} \sigma_{ml}(t, \hat{y}) \frac{\partial \sigma_{il}(t, \hat{y})}{\partial \hat{y}_m}$$

and $\mathcal{J}_{kl}^{(j)}$ are iterated stochastic integrals. Building upon these ideas, higher-order approximations for SDEs utilize expansions based on the set $\mathcal{M}$ of all multi-indices $\alpha = (j_1, \dots, j_l)$, iterated integrals $\mathcal{J}_{\alpha,s,t}$, and differential operators L^j. Defining the index set

$$\begin{aligned}
A_m = \{\alpha \in \mathcal{M} : l(\alpha) \geq 2 &\text{ and either } l(\alpha) + n(\alpha) \leq m \\
&\text{or } l(\alpha) = n(\alpha) = \tfrac{m+1}{2}\}
\end{aligned} \tag{12}$$

Here, $l(\alpha)$ denotes the length of the multi-index and $n(\alpha)$ denotes the number of zero indices in the multi-index α. The Itô differential operators, which play a key role in the stochastic Taylor expansions, are given by:

$$L^0 = \frac{\partial}{\partial t} + \sum_{k=1}^{M} c_k \frac{\partial}{\partial \hat{y}_k} + \frac{1}{2} \sum_{k,l=1}^{M} \sum_{j=1}^{q} \sigma_{kj} \sigma_{lj} \frac{\partial^2}{\partial \hat{y}_k \partial \hat{y}_l} \tag{13}$$

$$L^j = \sum_{k=1}^{M} \sigma_{kj} \frac{\partial}{\partial \hat{y}_k} \qquad j \in \{1, \dots, q\} \tag{14}$$

Accordingly, the Taylor approximation of order $\gamma = \frac{m}{2}$ can be expressed as:

$$\begin{aligned}
\hat{y}_i^{(j+1)} = \hat{y}_i^{(j)} &+ c_i(jh, \hat{y}^{(j)})h + \sum_{k=1}^{M} \sigma_{ik}(jh, \hat{y}^{(j)}) \Delta Z_k^{(j)} \\
&+ \sum_{\alpha \in A_m} f_{\alpha,i}(jh, \hat{y}^{(j)}) \mathcal{J}_{\alpha, jh, (j+1)h}
\end{aligned} \tag{15}$$

where the coefficient functions $f_{\alpha,i}$ are defined recursively such that $f_v = \hat{y}$ for the zero-length multi-index v, and $f_{j\alpha} = L^j f_\alpha$ for $j = 0, \dots, q$.

In the following section, we demonstrate how these expansions are applied to construct numerical schemes achieving strong convergence of order $\frac{3}{2}$ for SDEs. We also detail the approximation of iterated stochastic integrals and describe how perturbation and coupling methods are implemented to generate the required random variables for higher-order discretization.

2.3 Construction of an Explicit Strong Order $\frac{3}{2}$ Scheme for Stochastic Differential Equations

High-order strong schemes for SDEs rely on the stochastic Taylor expansion, where higher-order accuracy is achieved by systematically incorporating iterated stochastic integrals. Using relations (12) and (15) and specializing in $m = 3$ with the structure of A_m, we derive an explicit method that achieves strong order $\frac{3}{2}$. The resulting Taylor scheme takes the form

$$
\begin{aligned}
\hat{y}^{(j+1)} &= \hat{y}^{(j)} + c\,h + \sum_{k=1}^{M} \sigma_k\,\Delta Z^k \\
&+ \frac{1}{2\sqrt{h}} \sum_{l=0}^{M}\sum_{k=1}^{M}\Big[\sigma_l(jh,\Lambda_+^k) - \sigma_l(jh,\Lambda_-^k)\Big]\mathcal{J}_{(k,l)} \\
&+ \frac{1}{h}\sum_{k=0}^{M}\Big[\sigma_k((j+1)h,\hat{y}^{(j)}) - \sigma_k\Big]\mathcal{J}_{(0,k)} \\
&+ \frac{1}{2h}\sum_{l=0}^{M}\sum_{k=1}^{M}\Big[\sigma_l(jh,\Lambda_+^k) - 2\sigma_l + \sigma_l(jh,\Lambda_-^k)\Big]\mathcal{J}_{(0,l)} \\
&+ \frac{1}{2h}\sum_{k,l,r=1}^{M}\Big[\sigma_r(jh,\Psi_+^{(k,l)}) - \sigma_r(jh,\Psi_-^{(k,l)}) \\
&- \sigma_r(jh,\Lambda_+^k) + \sigma_r(jh,\Lambda_-^k)\Big]\mathcal{J}_{(k,l,r)}
\end{aligned} \tag{16}
$$

The auxiliary variables are defined as

$$
\begin{aligned}
\Lambda_\pm^k &= \hat{y}^{(j)} + \frac{1}{M}\,c\,h \pm \sigma_k\sqrt{h} \\
\Psi_\pm^{(k,l)} &= \Lambda_+^k \pm \sigma_l(jh,\Lambda_+^k)\sqrt{h}
\end{aligned} \tag{17}
$$

In multidimensional settings, achieving a strong order of convergence $\frac{3}{2}$ requires evaluating high-dimensional iterated stochastic integrals such as $\mathcal{J}_{(l,k)}$, $\mathcal{J}_{(0,k)}$, $\mathcal{J}_{(l,0)}$, and $\mathcal{J}_{(s,l,k)}$. These integrals rarely admit closed-form expressions and are computationally demanding to approximate directly. To overcome this difficulty, each $\mathcal{J}_\alpha$ is approximated by a randomized surrogate expressed as a sum of products of independent standard normal random variables, designed to match the required statistical moments:

$$
\mathcal{J}_\alpha = h^{\frac{l(\alpha)+n(\alpha)}{2}} \sum_{\beta=(i_1,\ldots,i_l)} K_\beta \prod_{k:\, i_k<j_k} U_{j_k} \tag{18}
$$

where the summation extends over all tuples β satisfying $i_k = j_k$ or $i_k = 0 < j_k$, and where $K_\beta, U_k \sim \mathcal{N}(0,1)$ are independent. In this construction, defining $\epsilon = h^{1/2}$ and $\mathcal{M}_m = \{\alpha \in \mathcal{M} : 2 \le l(\alpha) \le m\}$, the random component of a single step can be expressed as follows:

$$
Y_i = \epsilon \sum_{k=1}^{M} \sigma_{ik}(0,\hat{y}^{(0)})U_k + \theta_i\Big(\epsilon, U, (\epsilon^{l(\alpha)}K_\alpha)_{\alpha\in\mathcal{M}_m}\Big) \tag{19}
$$

where θ_i is a polynomial whose monomials are at least second order in ϵ. To improve efficiency, a perturbative replacement $K_\beta \mapsto W_\beta$ with $W_\alpha \sim \mathcal{N}(0,1)$ independent is employed, producing the simulatable surrogate

$$
\bar{\mathcal{J}}_\alpha = h^{\frac{l(\alpha)+n(\alpha)}{2}} \sum_{\beta=(i_1,\ldots,i_l)} W_\beta \prod_{k:\, i_k<j_k} \bar{U}_{j_k} \tag{20}
$$

and thus

$$
\bar{Y}_i = \epsilon \sum_{k=1}^{M} \sigma_{ik}(0,\hat{y}^{(0)})\bar{U}_k + \theta_i\Big(\epsilon, \bar{U}, (\epsilon^{l(\alpha)}W_\alpha)_{\alpha\in\mathcal{M}_m}\Big) \tag{21}
$$

To formalize the coupling argument, we use the following theorem adapted from [7].

Theorem 2.1 *Assume that the matrix (σ_{ik}) has rank q. Suppose that the random variables W_α have all finite moments and satisfy $\mathbb{E}(K_{\alpha_1}\cdots K_{\alpha_r}) = \mathbb{E}(W_{\alpha_1}\cdots W_{\alpha_r})$ whenever $\alpha_1,\ldots,\alpha_r \in \mathcal{M}_m$ and $\sum_{k=1}^{M}(l(\alpha_k)-1) \le m-1$. Then for $p \ge 2$, $\mathbb{B}_p(Y,\bar{Y}) \le C\,\epsilon^{m+1}$, where the constant C depends only on M, m, upper bounds for the constants σ_{ik}, $f_{\alpha,i}$, and a right inverse of the matrix (σ_{ik}), and moment bounds for W_α.*

Under the regularity assumptions on the drift and diffusion coefficients—boundedness of the functions and their derivatives up to second order, and a diffusion matrix of full rank with a uniformly bounded right inverse—the iterated integrals in (16) can be replaced by their simulatable counterparts without loss of accuracy. Substituting each $\mathcal{J}_\alpha$ with $\bar{\mathcal{J}}_\alpha$ yields the explicit, strongly convergent step of order $\frac{3}{2}$:

$$
\begin{aligned}
\hat{y}^{(j+1)} &= \hat{y}^{(j)} + c\,h + \sum_{k=1}^{M} \sigma_k\,\Delta Z^k \\
&+ \frac{1}{2\sqrt{h}} \sum_{l=0}^{M}\sum_{k=1}^{M}\Big[\sigma_l(jh,\Lambda_+^k) - \sigma_l(jh,\Lambda_-^k)\Big]\bar{\mathcal{J}}_{(k,l)} \\
&+ \frac{1}{h}\sum_{k=0}^{M}\Big[\sigma_k((j+1)h,\hat{y}^{(j)}) - \sigma_k\Big]\bar{\mathcal{J}}_{(0,k)} \\
&+ \frac{1}{2h}\sum_{l=0}^{M}\sum_{k=1}^{M}\Big[\sigma_l(jh,\Lambda_+^k) - 2\sigma_l + \sigma_l(jh,\Lambda_-^k)\Big]\bar{\mathcal{J}}_{(0,l)} \\
&+ \frac{1}{2h}\sum_{k,l,r=1}^{M}\Big[\sigma_r(jh,\Psi_+^{(k,l)}) - \sigma_r(jh,\Psi_-^{(k,l)}) \\
&- \sigma_r(jh,\Lambda_+^k) + \sigma_r(jh,\Lambda_-^k)\Big]\bar{\mathcal{J}}_{(k,l,r)}
\end{aligned} \tag{22}
$$

This randomized substitution maintains the strong order $\frac{3}{2}$ while eliminating the explicit computation of multidimensional integrals, thus producing an efficient and scalable scheme for practical simulation.

The surrogate integrals $\bar{\mathcal{J}}_\alpha$ follow directly from (20):

$$
\bar{\mathcal{J}}_{lk} = h\Big(\tfrac{1}{2}\bar{U}_l\bar{U}_k + W_{0k}\bar{U}_l - W_{0l}\bar{U}_k + W_{lk}\Big) \tag{23}
$$

$$
\bar{\mathcal{J}}_{0k} = h^{\frac{3}{2}}\Big(\tfrac{1}{2}\bar{U}_k + W_{0k}\Big) \tag{24}
$$

$$
\bar{\mathcal{J}}_{00} = \tfrac{h^2}{2} \tag{25}
$$

$$
\bar{\mathcal{J}}_{l0} = h^{\frac{3}{2}}\Big(\tfrac{1}{2}\bar{U}_l - W_{0l}\Big) \tag{26}
$$

$$
\bar{\mathcal{J}}_{rlk} = \tfrac{h^{\frac{3}{2}}}{6}\big(\bar{U}_r\bar{U}_l\bar{U}_k - \delta_{lk}\bar{U}_r - \delta_{rk}\bar{U}_l - \delta_{rl}\bar{U}_k\big) \tag{27}
$$

for $k, l, r > 0$, where $\{\bar{U}_k\}_{k=1}^M$ and $\{W_{kl}\}_{k,l=1}^M$ are mutually independent standard normal random variables, and

δ_{lk}, δ_{rk}, and δ_{rl} denote the Kronecker delta. The statistical moments of the variables in (23)–(27) are essential to ensure that the surrogate integrals retain the correct weak and strong properties of the true stochastic integrals. These moments are obtained using Lemmas 2.2–2.4 in [6], which establish the required deterministic and antisymmetric properties of the reference variables W_β.

The coupling framework of Theorem 2.1 is employed to quantify the approximation error introduced by this replacement.

If the auxiliary variables K_β satisfy the required moment conditions

$$\mathbb{E}(K_{\alpha_1}\cdots K_{\alpha_r}) = \mathbb{E}(W_{\alpha_1}\cdots W_{\alpha_r}) \quad \text{for all } \alpha_1,\ldots,\alpha_r \in \mathcal{M}_m \text{ with } \sum_{k=1}^{M}(l(\alpha_k)-1) \le m-1 \tag{28}$$

then the Wasserstein bound between Y and $\bar{Y}$ ensures the existence of a coupling satisfying

$$\mathbb{B}_p(Y,\bar{Y}) \le C(p)\, h^{\frac{m+1}{2}} \tag{29}$$

which confirms that the surrogate integrals preserve the strong convergence order uniformly in time. For $m = 3$, the random variables W_α must reproduce the moments $\mathbb{E}(W_\alpha)$ for all α of length two and three (with nonzero indices), as well as the mixed moments $\mathbb{E}(W_\alpha W_\beta)$ for pairs of indices α, β of length two. These requirements ensure the consistency of the modified integrals $\bar{\mathcal{J}}_\alpha$ and guarantee the theoretical order of accuracy of the proposed scheme. The following lemmas summarize the necessary moment conditions for the reference variables K_β, which the random variables W_β are designed to satisfy.

Lemma 2.2 *Let $\beta = (jj\ldots j)$ be a sequence with length $l \ge 2$. Then: (i) if $j = 0$, then $W_\beta = \frac{1}{l!}$; and (ii) if $j > 0$, then $W_\beta = 0$ when l is odd, and $W_\beta = \frac{(-1)^r}{2^r r!}$ when $l = 2r$.*

Proof. For a detailed proof, see Lemma 5 in [6].

Lemma 2.3 *If $\beta_1,\ldots,\beta_e \in \mathcal{N}$ and a given $j \ge 1$ appear an odd number of times in the concatenated multi-index $\beta_1\ldots\beta_e$, then $\mathbb{E}(W_{\beta_1}\ldots W_{\beta_e}) = 0$.*

Proof. This result can be found in Lemma 6 of [6].

Lemma 2.4 *(i) If $0 \le k < l$, then $W_{lk} = -W_{kl}$ and $\mathbb{E}(W_{kl}^2) = \frac{1}{12}$. (ii) If $k > 0$, then $\mathbb{E}(W_{0kk}) = \mathbb{E}(W_{k0k}) = \mathbb{E}(W_{kk0}) = -\frac{1}{6}$.*

Proof. For more details, refer to Lemma 7 in [6]. As a result, the moments in equation (27) are determined using Lemmas (2.2), (2.3), and (2.4):

Explicit values:

$$W_{00} = \frac{1}{2}$$
$$W_{000} = \frac{1}{6}$$
$$W_{kk} = \frac{1}{2}, \quad W_{kkk} = 0, \quad k > 0$$

Antisymmetry and zero mean:

$$W_{lk} = -W_{kl}, \quad \mathbb{E}(W_{kl}) = 0, \quad 0 \le k < l$$

High-order expectation properties:

$$\mathbb{E}(W_{rlk}) = 0, \quad k,l,r > 0$$
$$\mathbb{E}(W_{0kk}) = \mathbb{E}(W_{k0k}) = \mathbb{E}(W_{kk0}) = -\frac{1}{6}, \quad k > 0$$

Permutation-based zero expectation:

$$\mathbb{E}(W_\alpha) = 0, \quad \text{if } \alpha = 0kl \text{ or any permutation thereof, with } \quad 0 < k < l$$
$$\mathbb{E}(W_\alpha) = 0, \quad \text{if } \alpha = 00l \text{ or any permutation thereof, with } l > 0$$

Cross terms and variance:

$$\mathbb{E}(W_{kl}W_{k_1l_1}) = 0, \quad \text{if } k < l,\ k_1 < l_1,\ (k,l) \ne (k_1,l_1)$$
$$\mathbb{E}(W_{kl}^2) = \frac{1}{12}, \quad 0 \le k < l$$

In MATLAB, the random variables W_{kl} for $k < l$ can be generated from a normal distribution with zero mean and variance $\frac{1}{12}$, ensuring independence. This is one possible implementation; however, other constructions for the variables W_β are also admissible.

The required moment conditions are satisfied by enforcing the antisymmetry condition

$$W_{kl} = -W_{lk}, \quad 0 \le k < l$$

together with the deterministic assignments

$$W_{00} = \frac{1}{2}, \quad W_{kk} = \frac{1}{2}, \quad W_{000} = \frac{1}{6},$$
$$W_{0kk} = W_{k0k} = W_{kk0} = -\frac{1}{6}, \quad k > 0$$

and setting all remaining W_β of length three to zero.

In response to the request to present an algorithm (rather than code), we provide a full, stepwise algorithmic description aligned with the notation of the main text.

The following algorithm provides a concrete realization of the moment-matching construction for iterated stochastic integrals introduced above. Although the theoretical framework defines a family of auxiliary random variables $\{W_\beta\}$ in general form, only those components that contribute directly to the surrogate integrals $\bar{\mathcal{J}}_{lk}$, $\bar{\mathcal{J}}_{0k}$, and $\bar{\mathcal{J}}_{rlk}$ are required in the implementation. The remaining components (e.g., variables such as W_{000} and W_{0kk}) appear in the general formulation for completeness and consistency with the moment system, but do not enter explicitly into the numerical scheme since the corresponding stochastic integrals either vanish or reduce to deterministic quantities (e.g., $\bar{\mathcal{J}}_{00} = \frac{h^2}{2}$). This reduction is standard in high-order strong simulation methods and follows the practical implementation strategy used, for example, in the work of Davie [7] and Kloeden and Platen [11].

https://doi.org/10.57647/mathsci.2025.1903.15

2.4 Explicit Strong Order-$\frac{3}{2}$ Algorithm for Stochastic Differential Equations

Algorithmic 1. Explicit strong order-$\frac{3}{2}$ scheme for SDEs based on (17)–(22)

1: **Input:** drift $c(t,y) \in \mathbb{R}^q$, diffusion matrix $\sigma(t,y) = [\sigma_1,\dots,\sigma_M] \in \mathbb{R}^{q\times M}$, initial condition $\hat{y}^{(0)} \in \mathbb{R}^q$, final time $T > 0$, number of steps $N \in \mathbb{N}$.
2: **Out put:** trajectory $\{\hat{y}^{(j)}\}_{j=0}^{N}$.
3: Set the time step $h := T/N$; set $y \leftarrow \hat{y}^{(0)}$; store $\hat{y}^{(0)} \leftarrow y$.
4: **for** $j = 0, 1, \dots, N-1$ **do**
5: Set the current time $t \leftarrow jh$.
6: Evaluate drift and diffusion at (t, y):
$c \leftarrow c(t,y) \in \mathbb{R}^q, \quad \sigma \leftarrow \sigma(t,y) = [\sigma_1,\dots,\sigma_M] \in \mathbb{R}^{q\times M}$.
7: Draw independent Brownian increments $\Delta Z^{(k)} \sim \mathcal{N}(0,h)$ for $k = 1,\dots,M$.
8: Draw independent standard normals $U_k \sim \mathcal{N}(0,1)$ and $W_{0k} \sim \mathcal{N}(0,1)$ for each $k = 1,\dots,M$.
9: Construct an antisymmetric matrix $W = (W_{lk})_{1\le l,k\le M}$ as follows:
10: Set $W_{kk} := \frac{1}{2}$ for all $k = 1,\dots,M$.
11: For all $1 \le l < k \le M$:
sample W_{lk} with $\mathrm{Var}(W_{lk}) = \frac{1}{12}$ and set $W_{kl} := -W_{lk}$.
12: For each $k = 1,\dots,M$, define the auxiliary states
$\Lambda_{\pm}^{k} := y + \frac{1}{M}\, c\, h \pm \sigma_k(t,y)\sqrt{h}$.
13: For each ordered pair (k,l) with $1 \le k,l \le M$, define
$\Psi_{\pm}^{(k,l)} := \Lambda_{+}^{k} \pm \sigma_l\left(t, \Lambda_{+}^{k}\right)\sqrt{h}$.
14: Form the surrogate iterated integrals:
$\mathcal{J}_{lk} := h\left(\frac{1}{2}U_l U_k + W_{0k}U_l - W_{0l}U_k + W_{lk}\right)$
$\mathcal{J}_{0k} := h^{3/2}\left(\frac{1}{2}U_k + W_{0k}\right)$,
$\mathcal{J}_{00} := \frac{h^2}{2}$,
$\mathcal{J}_{l0} := h^{3/2}\left(\frac{1}{2}U_l - W_{0l}\right)$
$\mathcal{J}_{rlk} := \frac{h^{3/2}}{6}\left(U_r U_l U_k - \delta_{lk}U_r - \delta_{rk}U_l - \delta_{rl}U_k\right)$
for all $k,l,r \in \{1,\dots,M\}$, where $\delta_{lk}, \delta_{rk}, \delta_{rl}$ denote the Kronecker delta.
15: Compute the base increment (Euler part):
$\mathrm{incr} \leftarrow c\,h + \sum_{k=1}^{M} \sigma_k\, \Delta Z^{(k)}$. 16: Add the order -$\frac{3}{2}$ corrections as in (22):
$\mathrm{incr} \leftarrow \mathrm{incr} + \frac{1}{2\sqrt{h}} \sum_{l=1}^{M}\sum_{k=1}^{M}$
$\left[\sigma_l\left(t,\Lambda_{+}^{k}\right) - \sigma_l\left(t,\Lambda_{-}^{k}\right)\right] \mathcal{J}_{lk}$
$+\frac{1}{h}\sum_{k=1}^{M}$
$\left[\sigma_k(t+h,y) - \sigma_k(t,y)\right] \mathcal{J}_{0k}$
$+\frac{1}{2h}\sum_{l=1}^{M}\sum_{k=1}^{M} \left[\sigma_l\left(t,\Lambda_{+}^{k}\right) - 2\,\sigma_l(t,y) + \sigma_l\left(t,\Lambda_{-}^{k}\right)\right] \mathcal{J}_{0l}$
$+\frac{1}{2h}\sum_{k=1}^{M}\sum_{l=1}^{M}\sum_{r=1}^{M} \left[\sigma_r\left(t,\Psi_{+}^{(k,l)}\right) - \sigma_r\left(t,\Psi_{-}^{(k,l)}\right)\right.$
$\left.-\sigma_r\left(t,\Lambda_{+}^{k}\right) + \sigma_r\left(t,\Lambda_{-}^{k}\right)\right] \mathcal{J}_{rlk}$
17: Update the state $y \leftarrow y + \mathrm{incr}$ and store $\hat{y}^{(j+1)} \leftarrow y$.
18: **end for**

This algorithmic description is a direct implementation of the strong order-$\frac{3}{2}$ scheme derived in equations (17)–(22) and the surrogate iterated integrals (23)–(27). A brief theoretical time-complexity analysis is added below to quantify the per-step and total computational cost of the proposed scheme.

2.5 Computational Complexity Analysis

The explicit strong order-$\frac{3}{2}$ scheme balances accuracy with computational efficiency. Let q denote the dimension of the state vector and M the dimension of the driving Wiener process. During each time step, the algorithm performs several operations whose computational cost can be characterized as follows:

- Evaluation of the drift vector $c(t,y) \in \mathbb{R}^q$;
- Evaluation of the diffusion matrix $\sigma(t,y) \in \mathbb{R}^{q\times M}$ at multiple auxiliary states;
- Construction of the intermediate states $\Lambda_{\pm}^{k}$, which requires $O(M)$ evaluations per k and therefore $O(M^2)$ total work;
- Construction of the auxiliary states $\Psi_{\pm}^{(k,l)}$ for all ordered pairs (k,l), contributing another $O(M^2)$ evaluations;
- Assembly of the correction terms involving triple summations over (k,l,r), which yields a worst-case arithmetic complexity of $O(M^3)$.

Combining these contributions, the overall computational effort per time step satisfies

$$C_{\text{step}} = O(qM^3), \qquad C_{\text{total}} = O(N\,qM^3).$$

In many practical scenarios, the effective computational cost is lower than this upper bound. This reduction arises from reusing intermediate quantities, the antisymmetric structure of the random matrix $W = (W_{lk})$, and structural properties of the diffusion matrix such as sparsity or low rank in high-dimensional systems. Under such conditions, the empirical complexity often behaves closer to $O(qM^2)$, making the method highly competitive.

It is worth noting that classical schemes provide a useful baseline for comparison. The Euler–Maruyama method has a per-step complexity of only $O(qM)$ but achieves a substantially lower strong convergence order of $O(h^{1/2})$. First-order methods derived from the Itô–Taylor expansion improve the rate to $O(h)$, yet their practical implementation typically involves explicit evaluation of stochastic iterated integrals, whose computational burden increases significantly as the dimension M grows.

In contrast, the proposed strong order-$\frac{3}{2}$ scheme attains higher accuracy without computing any explicit iterated stochastic integrals. These terms are replaced by moment-matched random variables, preserving the correct statistical properties while maintaining a tractable computational structure. This leads to a favorable balance between accuracy and efficiency, making the method particularly suitable for multidimensional SDEs that require precise pathwise approximation.

2.6 Experimental Results

As requested, we include both (i) piecewise-linear plots of the approximate solutions and (ii) confidence intervals illustrating stochastic variability. Confidence intervals are constructed from independent trajectories at each time point.

https://doi.org/10.57647/mathsci.2025.1903.15

The following stochastic differential system was simulated using (17) and (22) with $N = 200$ time steps:

$$\begin{cases} dy_1 = \hat{y}_1\,dt + (\sin^2(\hat{y}_1)+1)\,dZ_t^1 - (\cos^2(\hat{y}_2))\,dZ_t^2 \\ d\hat{y}_2 = \dfrac{t+2}{1+\hat{y}_2^2}\,dt + (\cos^2(\hat{y}_1))\,dZ_t^1 + (\sin^2(\hat{y}_2)+1)\,dZ_t^2 \\ \hat{y}_1(0) = 1 \\ \hat{y}_2(0) = 2 \\ 0 \le t \le 1 \end{cases} \tag{30}$$

Figure 1 and Figure 2 together provide a comprehensive visualization, addressing the reviewer's requests to plot and tabulate the numerical solutions, illustrate the piecewise-linear curves, and include confidence bounds.

Figure 1 highlights the deterministic component of the approximation, where the piecewise-linear trajectories for $N = 200$ clearly depict the temporal evolution of the state variables using the proposed explicit order-$\frac{3}{2}$ method. In contrast, Figure 2 emphasizes the stochastic behavior by showing the 95% confidence intervals constructed from 100 independent realizations, thereby quantifying the uncertainty inherent in the numerical approximation. Together, these figures offer a holistic understanding of both the mean dynamics and the stochastic variability, demonstrating the robustness, reliability, and consistency of the proposed numerical approach.

Software Environment All numerical simulations and figures (Figure 1,Figure 2,Figure 3) were generated using **MATLAB R2014a**. All computations were performed with fixed random seeds to ensure reproducibility and the figures were produced using MATLAB's built-in visualization tools. This clarification ensures transparency and consistency in the computational environment used throughout the study.

3. Truncation Error

Consider the probability space $(\Omega, \mathcal{F}, \mathbb{P})$, where Ω denotes the set of all possible outcomes, $\mathcal{F}$ is a suitable σ-algebra of subsets of Ω, and $\mathbb{P}$ is the Wiener measure. Let $(\hat{y}^{(j)})_{j=1}^N$ be a sequence of approximate solutions to the stochastic differential equation (SDE) in (9), defined in this probability space. We say that this sequence converges in the L^p sense with order γ to the exact solution $(\hat{y}_{jh})_{j=1}^N$ at time T if there exist constants $C > 0$ and $\delta_0 > 0$ such that for all $h \in (0, \delta_0]$, we have

$$\left(\mathbb{E}\left(\max_{j=1}^{N} |\hat{y}^{(j)} - \hat{y}_{jh}|^p\right)\right)^{1/p} \le C(p)h^\gamma \tag{31}$$

To illustrate the difference between schemes, recall that the Euler scheme (10) achieves convergence order $\frac{1}{2}$:

$$\mathbb{E}\left(\max_{j=1}^{N} |\hat{y}^{(j)} - \hat{y}_{jh}|^p\right) = O(h^{p/2}) \tag{32}$$

while the Milstein scheme (11) achieves order 1:

$$\mathbb{E}\left(\max_{j=1}^{N} |\hat{y}^{(j)} - \hat{y}_{jh}|^p\right) = O(h^p) \tag{33}$$

Let us now introduce the metric for random vectors in $\mathbb{R}^{qN}$: define $\hat{y} = (\hat{y}^{(j)})_{j=1}^N$ and $\bar{y} = (\bar{y}^{(j)})_{j=1}^N$, both constructed on the same probability space. We set

$$G_{p,\infty} = \left(\mathbb{E}\left(\max_{j=1}^{N} |\hat{y}^{(j)} - \bar{y}^{(j)}|^p\right)\right)^{1/p} \tag{34}$$

This is a form of the Wasserstein distance, indicating the existence of a coupling in Ω that satisfies the aforementioned bound. Accordingly,

$$\mathbb{B}_{p,\infty}(\hat{y}, \bar{y}) = \inf G_{p,\infty}(\hat{y}, \bar{y}) \tag{35}$$

where the infimum is taken over all possible couplings of the distributions of $\hat{y}$ and $\bar{y}$. The above construction shows that an error bound of the form $\mathbb{B}_{p,\infty}(\hat{y}^{(j)}, \hat{y}_{jh}) = O(h^\gamma)$ leads to the existence of a random vector $\hat{u} = (\hat{u}^{(j)})_{j=1}^N$ on the same space, with the law of $(\hat{y}^{(j)})_{j=1}^N$, and $G_{p,\infty}(\hat{u}, \hat{y}_{jh}) = O(h^\gamma)$. In effect, simulating the numerical scheme may be seen as generating a random variable that strongly approximates the solution. We now connect this to the strong L^p error analysis and to the coupling provided by Theorem 2.1. Under standard regularity assumptions for the coefficients and the moment-matching condition:

$$\mathbb{E}(K_{\alpha_1}\cdots K_{\alpha_r}) = \mathbb{E}(W_{\alpha_1}\cdots W_{\alpha_r}) \qquad \text{whenever} \quad \sum_{k=1}^{M}(l(\alpha_k)-1) \le m-1$$

Theorem 2.1 ensures there exists a coupling between the true iterated-integral representation and its randomized surrogate, which yields the following L^p error bound for any time discretization step from $t = jh$ to $t = (j+1)h$ (for arbitrary $j = 0, 1, \ldots, N$):

$$\mathbb{E}\Bigg|\sum_{k=1}^{M} \sigma_{ik}\left(jh, \hat{y}^{(j)}\right) \epsilon\left(\bar{U}_k^{(j)} - U_k^{(j)}\right) + \sum_{\alpha\in A_m} f_\alpha\left(jh, \hat{y}^{(j)}\right)\left(\bar{\mathcal{J}}_{\alpha,jh,(j+1)h} - \mathcal{J}_{\alpha,jh,(j+1)h}\right)\Bigg|^p \le C(p)\,h^{\frac{p(m+1)}{2}}. \tag{36}$$

To propagate the error bound across multiple steps and to ensure comprehensive accuracy for the scheme, we employ a recursive approach. At each discretization step, the error is related to its predecessor through classical inequalities, which makes it possible to carry local estimates forward across the interval. Our analysis hinges on two foundational lemmas, essential for establishing the regularity and stability needed for the subsequent bounds.

Lemma 3.1 *Let $(\Omega, \mathcal{F}, \mathbb{P})$ be a probability space, and let c and σ be real-valued random variables. For $p \ge 2$, the following inequality holds:*

$$(\mathbb{E}|c+\sigma|^p)^{2/p} \le (\mathbb{E}|c|^p)^{2/p} + p^{2/p}\left|\mathbb{E}(\sigma c|c|^{p-2})\right|^{2/p} + \left(2^{p-1}(p-1) + 2^{p-2}p(p-1)\right)^{2/p}(\mathbb{E}|\sigma|^p)^{2/p} \tag{37}$$

https://doi.org/10.57647/mathsci.2025.1903.15

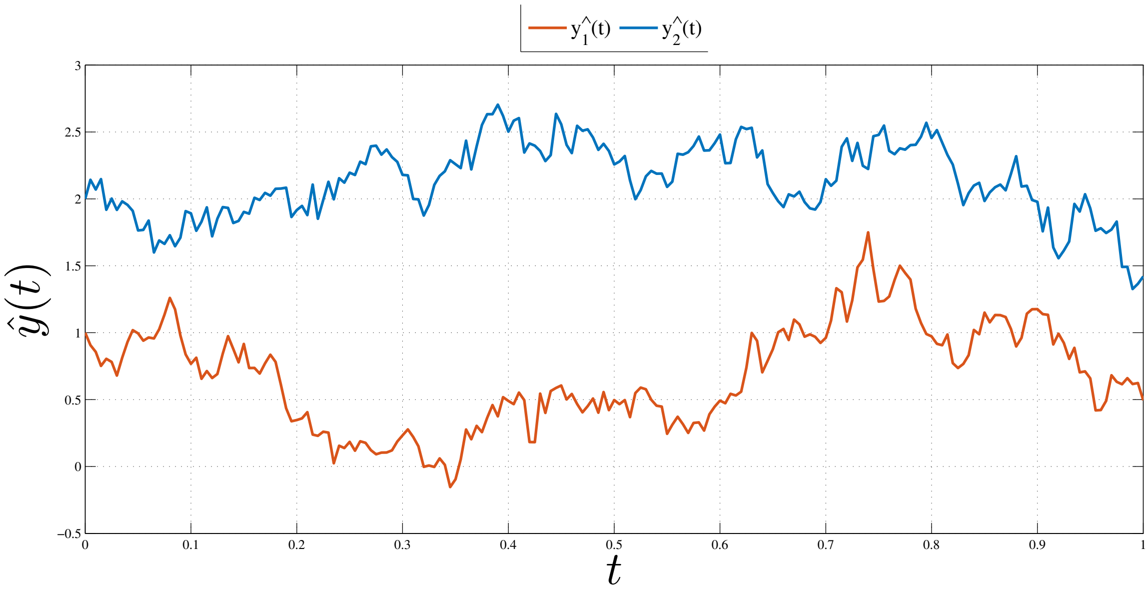

Figure 1. Piecewise-linear approximation of the numerical solutions $(\hat{y}_1, \hat{y}_2)$ over the interval $[0, 1]$ with $N = 200$ time steps. The trajectories demonstrate the discrete evolution of the state variables under the proposed explicit order-$\frac{3}{2}$ scheme.

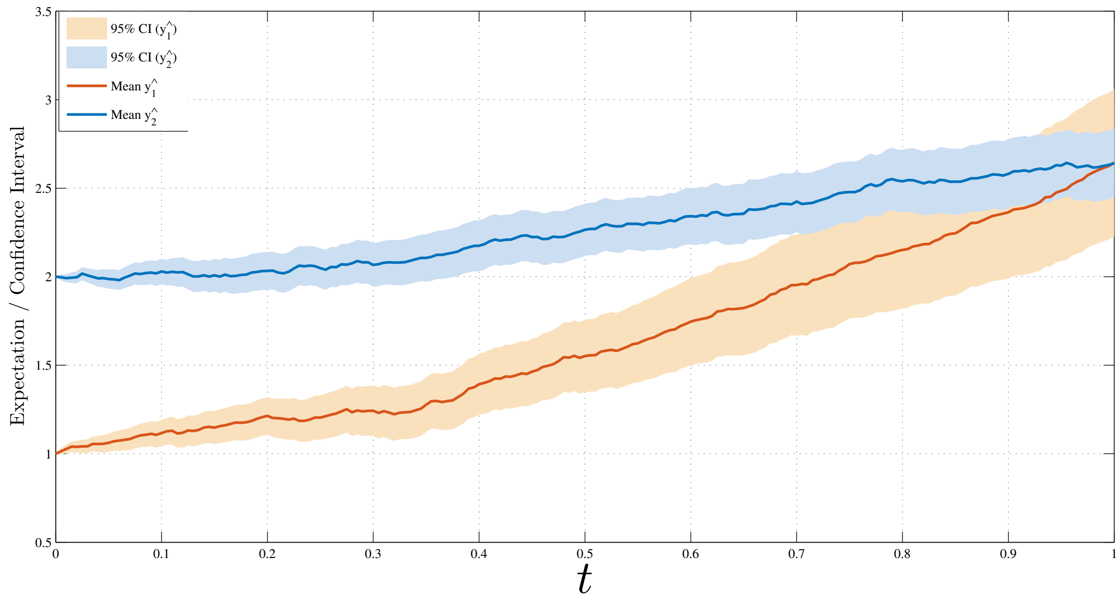

Figure 2. Numerical solutions with 95% confidence intervals computed from 100 independent Monte Carlo trajectories at each time point. The shaded regions illustrate the stochastic variability around the mean paths of $\hat{y}_1$ and $\hat{y}_2$, quantifying the reliability of the numerical results.

https://doi.org/10.57647/mathsci.2025.1903.15

Proof. Let $f(c+\sigma) = |c+\sigma|^p$. We expand this around c using the Taylor expansion:

$$f(c+\sigma) = f(c) + \sigma f'(c) + \sigma^2 \int_0^1 f''(c+\sigma t)(1-t)dt \tag{38}$$

Taking the expectation, we obtain $\mathbb{E}(|c+\sigma|^p) = \mathbb{E}(f(c)) + p\mathbb{E}(\sigma f'(c)) + \mathbb{E}(\sigma^2 \int_0^1 f''(c+\sigma t)(1-t)dt)$ where, $f(c) = |c|^p$, so $f'(c) = pc|c|^{p-2}$, while $f(c+\sigma t) = |c+\sigma t|^p$, so $f'(c+\sigma t) = p(c+\sigma t)|c+\sigma t|^{p-2}$ and the bound of f'' in the integral in the expansion is $f''(c+\sigma t) = p(p-1)|c+\sigma t|^{p-2} \leq 2^{p-2}p(p-1)\left[|c|^{p-2} + |\sigma|^{p-2}\right]$. By substituting this in the above expansion, we have

$$\begin{aligned}\mathbb{E}(|c+\sigma|^p)^{\frac{2}{p}} &\leq \Big[\mathbb{E}|c|^p + p\left|\mathbb{E}(\sigma c\,|c|^{p-2})\right| \\ &\quad + 2^{p-2}p(p-1)\,\mathbb{E}(\sigma^2|c|^{p-2}) \\ &\quad + 2^{p-2}p(p-1)\,\mathbb{E}|\sigma|^p\Big]^{\frac{2}{p}} \\ &\leq \Big[\mathbb{E}|c|^p + 2^{p-2}p(p-1)\,\mathbb{E}(\sigma^2|c|^{p-2})\Big]^{\frac{2}{p}} \\ &\quad + \Big[p\left|\mathbb{E}(\sigma c\,|c|^{p-2})\right| \\ &\quad + 2^{p-2}p(p-1)\,\mathbb{E}|\sigma|^p\Big]^{\frac{2}{p}} \end{aligned} \tag{39}$$

To establish a bound for the first term on the right-hand side (RHS), we utilize the following result: let g be a nonnegative function such that:

$$g(y) = y^{\frac{p}{2}} \tag{40}$$

where $g'(y) = \frac{p}{2}y^{\frac{p}{2}-1} \geq 0$ and $g''(y) = \frac{p}{2}(\frac{p}{2}-1)y^{\frac{p}{2}-2} \geq 0$ if y is nonnegative.
We expand (40) around $x = A$ by Taylor expansion, so we have

$$g(A+B) = g(A) + Bg'(A) + B^2 \int_0^1 g''(A+tB)(1-t)dt \tag{41}$$

where $B^2 \int_0^1 g''(A+tB)(1-t)dt = (\frac{p}{2}-1)(A+B)^{\frac{p}{2}} - (\frac{p}{2}-1)A^{\frac{p}{2}} - \frac{p}{2}BA^{\frac{p}{2}-1} \geq 0$.
Therefore, we have

$$(A+B)^{\frac{p}{2}} \geq A^{\frac{p}{2}} + \frac{p}{2}A^{\frac{p}{2}-1}B$$

where $A = \left(\mathbb{E}|c|^p\right)^{\frac{2}{p}}$ and $B = \left(2^{p-1}(p-1)\mathbb{E}|\sigma|^p\right)^{\frac{2}{p}}$.
Therefore,

$$\begin{aligned}(\mathbb{E}|c|^p)^{\frac{2}{p}} + \left(2^{p-1}(p-1)\,\mathbb{E}|\sigma|^p\right)^{\frac{2}{p}} &= A+B \\ \geq \left[\mathbb{E}|c|^p + \frac{p}{2}\left(\mathbb{E}|c|^p\right)^{1-\frac{2}{p}}\left(2^{p-1}(p-1)\,\mathbb{E}|\sigma|^p\right)^{\frac{2}{p}}\right]^{\frac{2}{p}}\end{aligned} \tag{42}$$

Using Holder's inequality in $\left(\mathbb{E}(\sigma^2|c|^{p-2}\right)$, we have $\left(\mathbb{E}(\sigma^2|c|^{p-2}\right) \leq \left(\mathbb{E}|c|^p\right)^{1-\frac{2}{p}}\left(\mathbb{E}|\sigma|^p\right)^{\frac{2}{p}}$ and, additionally, using the above result, we deduce the following

$$\begin{aligned}\mathbb{E}\left(|c+\sigma|^p\right)^{\frac{2}{p}} &\leq (\mathbb{E}|c|^p)^{\frac{2}{p}} + \left(2^{p-1}(p-1)\,\mathbb{E}|\sigma|^p\right)^{\frac{2}{p}} \\ &\quad + p^{\frac{2}{p}}\left|\mathbb{E}\left(\sigma c\,|c|^{p-2}\right)\right|^{\frac{2}{p}} \\ &\quad + \left(2^{p-2}p(p-1)\right)^{\frac{2}{p}}(\mathbb{E}|\sigma|^p)^{\frac{2}{p}} \\ &= (\mathbb{E}|c|^p)^{\frac{2}{p}} + p^{\frac{2}{p}}\left|\mathbb{E}\left(\sigma c\,|c|^{p-2}\right)\right|^{\frac{2}{p}} \\ &\quad + \Big(2^{p-1}(p-1) \\ &\quad + 2^{p-2}p(p-1)\Big)^{\frac{2}{p}}(\mathbb{E}|\sigma|^p)^{\frac{2}{p}}. \ \square \end{aligned} \tag{43}$$

Building on the above, we require precise control over the error in the approximated coefficients. The next lemma supplies essential bounds using Taylor expansion for smooth functions, under standard regularity and boundedness assumptions.

Lemma 3.2 *Assume that c and σ are continuous functions C^3 and uniformly bounded and that the derivatives up to order 3 are bounded. Then $\exists$ a constant $C > 0$ that is independent of $h > 0$, such that for each value of α, we have the following*

$$|f_{kl} - g_{kl}| \leq Ch \tag{44}$$

$$|f_{0l} - g_{0l}| \leq Ch^{\frac{1}{2}} \tag{45}$$

$$|f_{00} - g_{00}| \leq Ch \tag{46}$$

$$|f_{k0} - g_{k0}| \leq Ch \tag{47}$$

$$|f_{nkl} - g_{nkl}| \leq Ch^{\frac{1}{2}} \tag{48}$$

Proof. By $Y = O(h)$, we have $|Y| \leq Ch$ for fixed C. Let

$$\hat{y}^k_{\pm} = y + \frac{ch}{m} \pm \sigma_k\sqrt{h} \tag{49}$$

By expanding (49) twice around y; we have

$$\begin{aligned}\sigma_l(\hat{y}^k_+) &= \sigma_l(y) + \frac{h}{m}\sum_{i=1}^{q} c_i\frac{\partial\sigma_l}{\partial y_i} + \sqrt{h}\sum_{i=1}^{q}\sigma_{ik}\frac{\partial\sigma_l}{\partial y_i} \\ &\quad + \frac{h}{2}\sum_{i,j=1}^{q}\sigma_{ik}\sigma_{jk}\frac{\partial^2\sigma_l}{\partial y_i\partial y_j} + O(h^{\frac{3}{2}})\end{aligned} \tag{50}$$

and

$$\begin{aligned}\sigma_l(\hat{x}^k_-) &= \sigma_l(y) + \frac{h}{m}\sum_{i=1}^{q} c_i\frac{\partial\sigma_l}{\partial y_i} - \sqrt{h}\sum_{i=1}^{q}\sigma_{ik}\frac{\partial\sigma_l}{\partial y_i} \\ &\quad + \frac{h}{2}\sum_{i,j=1}^{q}\sigma_{ik}\sigma_{jk}\frac{\partial^2\sigma_l}{\partial y_i\partial y_j} + O(h^{\frac{3}{2}})\end{aligned} \tag{51}$$

Subtracting these expansions gives

$$\sigma_l(\hat{y}_+^k) - \sigma_l(\hat{y}_-^k) = 2\sqrt{h}\sum_{i=1}^{q}\sigma_{ik}\frac{\partial\sigma_l}{\partial y_i} + O(h^{\frac{3}{2}}) \quad (52)$$

Therefore,

$$\sum_{i=1}^{q}\sigma_{ik}\frac{\partial\sigma_l}{\partial y_i} = \frac{1}{2\sqrt{h}}[\sigma_l(\hat{y}_+^k) - \sigma_l(\hat{y}_-^k)] + O(h) \quad (53)$$

Hence, (44) is derived from this.
While adding these expansions gives

$$\begin{aligned}\sigma_l(\hat{y}_+^k) + \sigma_l(\hat{y}_-^k) = 2\sigma_l(y) + \frac{2h}{m}\sum_{i=1}^{q}c_i\frac{\partial\sigma_l}{\partial y_i} \\ +h\sum_{i,j=1}^{q}\sigma_{ik}\sigma_{jk}\frac{\partial^2\sigma_l}{\partial y_i\partial y_j} + O(h^{\frac{3}{2}})\end{aligned} \quad (54)$$

Thus,

$$\begin{aligned}\frac{\partial\sigma_l}{\partial t} + \frac{1}{m}\sum_{i=1}^{q}c_i\frac{\partial\sigma_l}{\partial y_i} + \frac{1}{2}\sum_{i,j=1}^{q}\sigma_{ik}\sigma_{jk}\frac{\partial^2\sigma_l}{\partial y_i\partial y_j} = \\ \frac{1}{2h}[\sigma_l(\hat{y}_+^k) - 2\sigma_l(y) + \sigma_l(\hat{y}_-^k)] + O(h^{\frac{1}{2}})\end{aligned} \quad (55)$$

Hence, (45) is derived from this.
The expansions for coefficient c are (by 1.5)

$$\begin{aligned}c(\hat{y}_+^k) = c(y) + \frac{h}{m}\sum_{i=1}^{q}c_i\frac{\partial c}{\partial y_i} + \sqrt{h}\sum_{i=1}^{l}\sigma_{ik}\frac{\partial c}{\partial y_i} \\ + \frac{h}{2}\sum_{i,j=1}^{q}\sigma_{ik}\sigma_{jk}\frac{\partial^2 c}{\partial y_i\partial y_j} + O(h^{\frac{3}{2}})\end{aligned} \quad (56)$$

and

$$\begin{aligned}c(\hat{y}_-^k) = c(y) + \frac{h}{m}\sum_{i=1}^{q}c_i\frac{\partial c}{\partial y_i} - \sqrt{h}\sum_{i=1}^{q}\sigma_{ik}\frac{\partial c}{\partial y_i} \\ + \frac{h}{2}\sum_{i,j=1}^{q}\sigma_{ik}\sigma_{jk}\frac{\partial^2 c}{\partial y_i\partial y_j} + O(h^{\frac{3}{2}})\end{aligned} \quad (57)$$

Therefore,

$$c(\hat{y}_+^k) - c(\hat{y}_-^k) = 2\sqrt{h}\sum_{i=1}^{q}\sigma_{ik}\frac{\partial c}{\partial y_i} + O(h^{\frac{3}{2}}) \quad (58)$$

Thus,

$$\sum_{i=1}^{l}\sigma_{ik}\frac{\partial c}{\partial y_i} = \frac{1}{2\sqrt{h}}[c(\hat{y}_+^k) - c(\hat{y}_-^k)] + O(h) \quad (59)$$

Therefore, (47) is derived from this.
However, adding expansions (56) and (57) will give us the following

$$\begin{aligned}c(\hat{y}_+^k) + c(\hat{y}_-^k) = 2c(y) + \frac{2h}{m}\sum_{i=1}^{q}c_i\frac{\partial c}{\partial y_i} \\ + h\sum_{i,j=1}^{q}\sigma_{ik}\sigma_{jk}\frac{\partial^2 c}{\partial y_i\partial y_j} + O(h^{\frac{3}{2}})\end{aligned} \quad (60)$$

Therefore,

$$\begin{aligned}\frac{\partial c}{\partial t} + \frac{1}{m}\sum_{i=1}^{q}c_i\frac{\partial c}{\partial y_i} + \frac{1}{2}\sum_{i,j=1}^{q}\sigma_{ik}\sigma_{jk}\frac{\partial^2 c}{\partial y_i\partial y_j} = \\ \frac{1}{2h}[c(\hat{y}_+^k) - 2c(y) + c(\hat{y}_-^k)] + O(h^{\frac{1}{2}})\end{aligned} \quad (61)$$

Thus, (46) is proved from this.
Now, we expand the following

$$\hat{\Psi}_{\pm}^{(k,l)} = \hat{y}_+^k \pm \sigma_l(\hat{y}_+^k)\sqrt{h} \quad (62)$$

where $\hat{y}_+^k$ is defined in (49).
Initially, we need to calculate the inner expansion $\sigma_l(\hat{y}_+^k)$ and substitute in (62); then find the whole expansion $\sigma_s(\Psi_{\pm}^{(k,l)})$

$$\sigma_l(\hat{y}_+^k) = \sigma_l(y) + \sqrt{h}\sum_{i=1}^{q}\sigma_{ik}\frac{\partial\sigma_l}{\partial y_i} + O(h) \quad (63)$$

Multiplying by $\sqrt{h}$ gives

$$\sqrt{h}\sigma_l(\hat{y}_+^k) = \sigma_l(y)\sqrt{h} + h\sum_{i=1}^{q}\sigma_{ik}\frac{\partial\sigma_l}{\partial y_i} + O(h^{\frac{3}{2}}) \quad (64)$$

Putting (64) in (62) and calculating the expansion

$$\hat{\Psi}_{\pm}^{(k,l)} = \hat{y}_+^k \pm (\sigma_l(y)\sqrt{h} + h\sum_{i=1}^{q}\sigma_{ik}\frac{\partial\sigma_l}{\partial y_i}) \quad (65)$$

The first expansion

$$\begin{aligned}\sigma_r(\hat{\Psi}_+^{(k,l)}) = \sigma_r(y) + \frac{h}{m}\sum_{z=1}^{q}c_z\frac{\partial\sigma_r}{\partial y_z} \\ + \sqrt{h}\sum_{z=1}^{q}\sigma_{zk}\frac{\partial\sigma_r}{\partial y_z} \\ + \sqrt{h}\sum_{z=1}^{q}\sigma_{zl}\frac{\partial\sigma_r}{\partial y_z} \\ + h\sum_{z=1}^{q}(\sum_{i=1}^{q}\sigma_{ik}\frac{\partial\sigma_l}{\partial y_i})_z\frac{\partial\sigma_r}{\partial y_z} \\ + \frac{h}{2}\sum_{z,e=1}^{q}\sigma_{zk}\sigma_{ek}\frac{\partial^2\sigma_r}{\partial y_z\partial y_e} \\ + \frac{h}{2}\sum_{z,e=1}^{q}\sigma_{zl}\sigma_{el}\frac{\partial^2\sigma_r}{\partial y_z\partial y_e} \\ + h(\sum_{z,e=1}^{q}\sigma_{zk}\sigma_{el}\frac{\partial^2\sigma_r}{\partial y_z\partial y_e} \\ + \sum_{z,e=1}^{q}\sigma_{ek}\sigma_{zl}\frac{\partial^2\sigma_r}{\partial y_z\partial y_e}) + O(h^{\frac{3}{2}})\end{aligned} \quad (66)$$

The second expansion w.r.t minus is In addition, we need to calculate the expansion of $\sigma_r(\hat{y}_{\pm}^l)$; where $\hat{y}_{\pm}^l = y + \frac{ch}{m} \pm \sigma_l\sqrt{h}$

$$\begin{aligned}\sigma_r(\hat{y}_+^l) = \sigma_r(y) + \frac{h}{m}\sum_{z=1}^{q}c_z\frac{\partial\sigma_r}{\partial y_z} + \sqrt{h}\sum_{z=1}^{q}\sigma_{zl}\frac{\partial\sigma_r}{\partial y_z} \\ + \frac{h}{2}\sum_{z,e=1}^{q}\sigma_{zl}\sigma_{el}\frac{\partial^2\sigma_r}{\partial y_z\partial y_e} + O(h^{\frac{3}{2}})\end{aligned} \quad (67)$$

https://doi.org/10.57647/mathsci.2025.1903.15

and

$$\sigma_r(\hat{y}^l_-) = \sigma_r(y) + \frac{h}{m}\sum_{z=1}^{q} c_z \frac{\partial \sigma_r}{\partial y_z} - \sqrt{h}\sum_{z=1}^{q}\sigma_{zl}\frac{\partial \sigma_r}{\partial y_z} + \frac{h}{2}\sum_{z,e=1}^{q}\sigma_{zl}\sigma_{el}\frac{\partial^2\sigma_r}{\partial y_z \partial y_e} + O(h^{\frac{3}{2}}) \quad (68)$$

Combining these expansions resulted

$$\sigma_r(\hat{\Psi}^{(k,l)}_+) - \sigma_r(\hat{\Psi}^{(k,l)}_-) - \sigma_r(\hat{y}^l_+) + \sigma_r(\hat{y}^l_-) = 2h\sum_{z=1}^{q}(\sum_{i=1}^{q}\sigma_{ik}\frac{\partial \sigma_l}{\partial y_i})_z\frac{\partial \sigma_r}{\partial y_z} + 2h(\sum_{z,e=1}^{q}\sigma_{zk}\sigma_{el}\frac{\partial^2\sigma_r}{\partial y_z\partial y_e} + \sum_{z,e=1}^{q}\sigma_{ek}\sigma_{zl}\frac{\partial^2\sigma_r}{\partial y_z\partial y_e}) + O(h^{\frac{3}{2}}) \quad (69)$$

Therefore,

$$\sum_{z=1}^{q}(\sum_{i=1}^{q}\sigma_{ik}\frac{\partial \sigma_l}{\partial y_i})_z\frac{\partial \sigma_r}{\partial y_z} + (\sum_{z,e=1}^{q}\sigma_{zk}\sigma_{el}\frac{\partial^2\sigma_r}{\partial y_z\partial y_e} + \sum_{z,e=1}^{q}\sigma_{ek}\sigma_{zl}\frac{\partial^2\sigma_r}{\partial y_z\partial y_e}) = \frac{1}{2h}[\sigma_r(\hat{\Psi}^{(k,l)}_+) - \sigma_r(\hat{\Psi}^{(k,l)}_-) - \sigma_r(\hat{y}^l_+) + \sigma_r(\hat{y}^l_-)] + O(h^{\frac{1}{2}}) \quad (70)$$

Thus, relation (48) follows immediately. By combining equations (53)–(70) and multiplying by the corresponding term $\bar{\mathcal{J}}\alpha$, we arrive at the estimate

$$\mathbb{E}\left|g_\alpha(jh,\hat{y}^{(j)})\bar{\mathcal{J}}_\alpha - f_\alpha(jh,\hat{y}^{(j)})\bar{\mathcal{J}}_\alpha\right|^p \le Ch^{\frac{p(m+1)}{2}} \quad (71)$$

From this, inequality (36) follows directly. As will be shown in equation (3), the coupling is constructed by following the same reasoning and technique employed in the original framework, with the distinction that, in the present case, it is developed specifically for g_α. The coefficient functions are evaluated at the random variables $\hat{y}^{(j)}$, such as $(U^{(j)}_k, K^{(j)}_\alpha)$ and $(\bar{U}^{(j)}_k, W^{(j)}_\alpha)$. The extended coupling between $(U^{(j)}_k, K^{(j)}_\alpha)$ and $(\bar{U}^{(j)}_k, W^{(j)}_\alpha)$ is conditional on the σ–algebra $\mathcal{F}_j = \sigma\{U_i, K_i, W_i : i < j\}$ at each time step, where $j = 0, 1, \ldots, N$. This construction introduces a sequential dependence among the couplings, where each coupling depends on the previous one—for example, the coupling at $j = 1$ is determined by the coupling at $j = 0$. To quantify this dependence and obtain an appropriate L^p–bound for the coupled increments, we take the expectation conditioned on $\mathcal{F}_j$, yielding the following conditional bound:

$$\mathbb{E}\left|\sum_{k=1}^{M}\sigma_{ik}(jh,\hat{y}^{(j)})\epsilon(\bar{U}^{(j)}_k - U^{(j)}_k) + \sum_{\alpha\in A_m} g_\alpha(jh,\hat{y}^{(j)})\bar{\mathcal{J}}_{\alpha,jh,(j+1)h} - \sum_{\alpha\in A_m} f_\alpha(jh,\hat{y}^{(j)})\mathcal{J}_{\alpha,jh,(j+1)h}\,\Big|\,\mathcal{F}_j\right|^p \le Ch^{\frac{p(m+1)}{2}}$$

From the nested expectation and the bounds provided in (36) and (71), we deduce:

$$\mathbb{E}\left|\sum_{k=1}^{M}\sigma_{ik}(jh,\hat{y}^{(j)})\epsilon(\bar{U}^{(j)}_k - U^{(j)}_k) + \sum_{\alpha\in A_m} g_\alpha(jh,\hat{y}^{(j)})\bar{\mathcal{J}}_{\alpha,jh,(j+1)h} - \sum_{\alpha\in A_m} f_\alpha(jh,\hat{y}^{(j)})\mathcal{J}_{\alpha,jh,(j+1)h}\right|^p \le Ch^{\frac{p(m+1)}{2}} \quad (72)$$

In practice, the error of the approximate solutions for this method is estimated statistically using computational tools. Since explicit analytical solutions for stochastic differential equations are rarely available, numerical accuracy is typically assessed by comparing simulations at different resolutions. However, empirical comparisons alone cannot fully characterize the convergence properties of a numerical scheme. Therefore, it is essential to complement these results with a rigorous theoretical framework that quantifies the approximation accuracy.

3.1 Weak Bound for Final Time

In this section, we establish a theoretical and numerical weak bound for the final-time approximation of the proposed strong order-$\frac{3}{2}$ scheme. The goal is to assess the weak accuracy of the numerical solution obtained from the explicit algorithm by quantifying the discrepancy between solutions computed with step sizes h and $h/2$.

3.1.1 Theoretical Weak Bound

Let $\hat{y}_h(T)$ and $\hat{y}_{h/2}(T)$ denote the numerical approximations of the true solution $\hat{y}(T)$ using step sizes h and $h/2$, respectively. By the Kantorovich–Rubinstein theorem, the weak error is bounded in terms of the 1-Wasserstein distance:

$$\begin{aligned}\sup_{f\in\mathrm{Lip}(1)} |\mathbb{E}f(\hat{y}_h) - \mathbb{E}f(\hat{y}_{h/2})| &= \mathbb{B}_1(\hat{y}_h, \hat{y}_{h/2}) \\ &= O(h^{3/2}) \quad (73)\end{aligned}$$

Here, Lip(1) denotes the class of all Lipschitz functions $f : \mathbb{R}^q \to \mathbb{R}$ satisfying $|f(u) - f(v)| \le |u - v|$ for all $u, v \in \mathbb{R}^q$. This ensures that the weak discrepancy between successive step-size approximations inherits the same asymptotic order as the strong convergence rate of the proposed scheme.

To verify this relation, note that for any coupling of $(\hat{y}_h, \hat{y}_{h/2})$ and any $f \in \mathrm{Lip}(1)$,

$$\begin{aligned}|\mathbb{E}f(\hat{y}_h) - \mathbb{E}f(\hat{y}_{h/2})| &\le \mathbb{E}|\hat{y}_h - \hat{y}_{h/2}| \Rightarrow \quad (74)\\ \sup_{f\in\mathrm{Lip}(1)} |\mathbb{E}f(\hat{y}_h) - \mathbb{E}f(\hat{y}_{h/2})| &\le \inf \mathbb{E}|\hat{y}_h - \hat{y}_{h/2}| \\ &= \mathbb{B}_1(\hat{y}_h, \hat{y}_{h/2})\end{aligned}$$

and equality follows by the Kantorovich–Rubinstein Theorem.

3.1.2 Weak Bound Simulation for Final Time

To numerically validate (73), the weak expectation $\mathbb{E}(f(\hat{y}_h))$ is approximated using a Monte Carlo procedure with $R = 3{,}000{,}000$ independent trajectories. We consider the Lipschitz-continuous test function

$$f(\hat{y}_1, \hat{y}_2) = |\hat{y}_1| + |\hat{y}_2|$$

evaluated at the final-time numerical approximations $\hat{y}_1$ and $\hat{y}_2$ obtained from the stochastic scheme.

The empirical mean and variance are computed as

$$\mathbb{E}(f(\hat{y}_h)) \approx \frac{1}{R}\sum_{r=1}^{R} f(\hat{y}_h^{(r)}),$$

$$\text{S.D.}(f(\hat{y}_h)) = \sqrt{\frac{1}{R-1}\sum_{r=1}^{R}\left(f(\hat{y}_h^{(r)}) - \mathbb{E}(f(\hat{y}_h))\right)^2}$$

To construct a confidence interval for the weak error, the expectation $\mathbb{E}(f(\hat{y}_h))$ is not analytically accessible, since the probability distribution of the solution is generally unknown. Therefore, it is standard in stochastic numerical analysis to approximate it by the empirical mean over R independent Monte Carlo trajectories:

$$\mathbb{E}(f(\hat{y}_h)) \approx \frac{1}{R}\sum_{r=1}^{R} f(\hat{y}_h^{(r)})$$

which is justified by the law of large numbers. This ensures convergence of the sample mean to the true expectation as R increases, providing a reliable basis for constructing confidence intervals of the weak error.

The standard error (S.E.) is estimated by

$$\text{S.E.} = \sqrt{\frac{\text{S.D.}(f(\hat{y}_h))^2 + \text{S.D.}(f(\hat{y}_{h/2}))^2}{R}}$$

For a 95% confidence level, the corresponding confidence interval (C.I.) is given by

$$\text{C.I.} = \Big[(\mathbb{E}(f(\hat{y}_h)) - \mathbb{E}(f(\hat{y}_{h/2}))) - 1.96 \times \text{S.E.},\\ (\mathbb{E}(f(\hat{y}_h)) - \mathbb{E}(f(\hat{y}_{h/2}))) + 1.96 \times \text{S.E.}\Big]$$

Table 1. Estimated truncation errors and 95% confidence intervals for the weak bound of the final-time approximation.

N	Truncation Error	95% Confidence Interval
2^9	0.0105	(0.0073, 0.0137)
2^{10}	0.0037	(0.0010, 0.0064)
2^{11}	0.0013	(0.0001, 0.0025)

Figure 3 illustrates the weak convergence behavior of the proposed explicit order-$\frac{3}{2}$ scheme. As observed, the weak error $\| \mathbb{E}[f(\hat{y}_h)] - \mathbb{E}[f(\hat{y}_{h/2})] \|$ decreases consistently as the step size h is refined, confirming the theoretically predicted rate of convergence. The least-squares regression line (orange dashed) exhibits a slope of approximately 1.61, which closely matches the expected order $O(h^{3/2})$. The shaded blue region represents the 95% confidence interval obtained through Monte Carlo simulations, showing that the variability in the weak error diminishes for smaller step sizes. The numerical results summarized in Table 1 correspond to these data points, providing quantitative evidence of truncation-error reduction and validating the reliability of the approximation at the final time $T = 1$.

These findings confirm the robustness and accuracy of the proposed explicit scheme for higher-order stochastic differential equations, demonstrating its suitability for reliable and efficient numerical simulation of multidimensional SDEs.

4. Conclusion

The numerical experiments confirm the theoretical convergence rate and validate the efficiency and reliability of the proposed strong order-$\frac{3}{2}$ scheme. The presented method effectively addresses the need for efficient and accurate numerical solutions for higher-order stochastic differential equations (SDEs), a challenge that remains insufficiently explored in the existing literature. The developed scheme enables strong approximations for multidimensional SDEs without imposing significant computational overhead. Moreover, the framework is flexible and can be systematically extended to achieve even higher-order strong approximations, such as order 2, by incorporating additional terms from the Itô–Taylor expansion. These potential extensions and their theoretical analyses will be the focus of future research. This conclusion has been reformulated to emphasize the main contributions, theoretical foundations, and potential applications of the proposed scheme, ensuring consistency with the overall structure and findings of the paper.

Acknowledgment

The Researchers would like to thank the Deanship of Graduate Studies and Scientific Research at Qassim University for financial support (QU-APC-2025)

Authors contributions

All the authors have participated sufficiently in the intellectual content, conception and design of this work or the analysis and interpretation of the data (when applicable), as well as the writing of the manuscript.

Availability of data and materials

The data that support the findings of this study are available from the corresponding author, upon reasonable request.

Conflict of interests

The author declare that they have no known competing financial interests or personal relationships that could have appeared to influence the work reported in this paper.

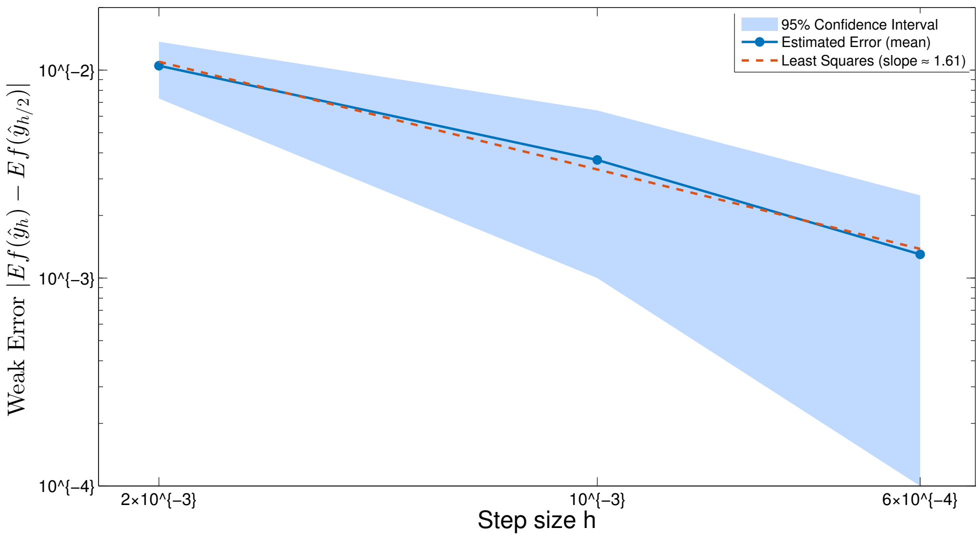

Figure 3. Weak bound for the final-time approximation (order $\frac{3}{2}$). The solid blue curve shows the estimated weak error versus the step size h on a log–log scale. The shaded region denotes the 95% confidence interval, and the orange dashed line represents the least-squares fit with slope ≈ 1.61, consistent with the theoretical rate $O(h^{3/2})$

References

1. Alfonsi A, Jourdain B, and Kohatsu-Higa A. Pathwise optimal transport bounds between a one-dimensional diffusion and its Euler scheme. The Annals of Applied Probability 2014; 24:1049–80. DOI: 10.1214/13-AAP941
2. Alfonsi A, Jourdain B, and Kohatsu-Higa A. Optimal transport bounds between the time-marginals of a multidimensional diffusion and its Euler scheme. arXiv preprint 2015. DOI: 10.48550/arXiv.1405.7007. arXiv: 1405.7007
3. Alves CJS and Cruzeiro AB. Monte Carlo simulation of stochastic differential systems – a geometrical approach. Stochastic Processes and their Applications 2008; 118:346–67. DOI: 10.1016/j.spa.2007.04.009
4. Cruzeiro AB and Malliavin P. Numerical approximation of diffusions in $\mathbb{R}^d$ using normal charts of a Riemannian manifold. Stochastic Processes and their Applications 2006; 116:1088–95. DOI: 10.1016/j.spa.2006.02.004
5. Davie A. KMT theory applied to approximations of SDE. *Springer Proceedings in Mathematics and Statistics*. Vol. 100. Springer, 2014 :185–201
6. Davie AM. Pathwise approximation of stochastic differential equations using coupling. Preprint. 2015
7. Davie AM. Polynomial perturbations of normal distributions. Preprint. 2017
8. Deya A, Neuenkirch A, and Tindel S. A Milstein-type scheme without Lévy area terms for SDEs driven by fractional Brownian motion. Annales de l'Institut Henri Poincaré Probabilités et Statistiques 2012; 48:518–50. DOI: 10.1214/10-AIHP392
9. Gelbrich M. Simultaneous time and chance discretization for stochastic differential equations. Journal of Computational and Applied Mathematics 1995; 58:255–89. DOI: 10.1016/0377-0427(94)00003-J
10. Gaines JG and Lyons TJ. Random generation of stochastic area integrals. SIAM Journal on Applied Mathematics 1994; 54:1132–46. DOI: 10.1137/S0036139992235706
11. Kloeden PE and Platen E. Numerical Solution of Stochastic Differential Equations. Berlin: Springer-Verlag, 1995
12. Wiktorsson M. Joint characteristic function and simultaneous simulation of iterated Itô integrals for multiple independent Brownian motions. The Annals of Applied Probability 2001; 11:470–87. DOI: 10.1214/aoap/1015345301
13. Rydén T and Wiktorsson M. On the simulation of iterated Itô integrals. Stochastic Processes and their Applications 2001; 91:151–68. DOI: 10.1016/S0304-4149(00)00053-3
14. Villani C. Topics in Optimal Transportation. American Mathematical Society, 2003
15. Alnafisah Y. A new order from the combination of exact coupling and the Euler scheme. AIMS Mathematics 2022; 7:6356–64. DOI: 10.3934/math.2022353

16. Alnafisah Y. The implementation comparison between the Euler and trivial coupling schemes for achieving strong convergence. AIMS Mathematics 2023; 8:29701–12. DOI: 10.3934/math.20231520

17. Barzegar N, Mirzaee F, and Solhi E. New technique based on Vieta–Lucas polynomials for solving nonlinear stochastic Itô–Volterra integral equation. International Journal of Numerical Modelling: Electronic Networks, Devices and Fields 2025; 38:e70044. DOI: 10.1002/jnm.70044

18. Mirzaee F, Naserifar S, and Solhi E. Meshless barycentric rational interpolation method for solving nonlinear stochastic fractional integro-differential equations. Iranian Journal of Science 2024; 48:709–33. DOI: 10.1007/s40995-024-01621-z

19. Solhi E, Mirzaee F, and Naserifar S. Enhanced moving least squares method for solving the stochastic fractional Volterra integro-differential equations of Hammerstein type. Numerical Algorithms 2024; 95:1921–51. DOI: 10.1007/s11075-023-01633-7

20. Mirzaee F, Solhi E, and Naserifar S. Accurate and stable numerical method based on the Floater–Hormann interpolation for stochastic Itô–Volterra integral equations. Numerical Algorithms 2023; 94:275–92. DOI: 10.1007/s11075-023-01500-5

21. Yari F, Mirzaee F, and Solhi E. A new spectral method using Mittag–Leffler wavelets for solving stochastic differential equations. Computational Methods for Differential Equations 2025. Articles in Press. DOI: 10.22034/CMDE.2025.66447.3101

22. Badawi H, Abu Arqub O, and Eid R. Theoretical predictions of existence and uniqueness for stochastic M-fractional differential models of random Brownian motion, exhibited with matrix spectral collocation solutions. Fractals 2025. DOI: 10.1142/S0218348X25403035

23. Badawi H, Abu Arqub O, and Shawagfeh N. Theoretical study and numerical analysis using the step spectral collocation method for stochastic M-fractional differential models of simplified Brownian motion within constant delays process. Journal of Applied Mathematics and Computing 2025; 71:6773–805. DOI: 10.1007/s12190-025-02523-y

24. Badawi H, Abu Arqub OA, and Shawagfeh N. Existence, uniqueness, and collocation solutions using the shifted Legendre spectral method for the Hilfer fractional stochastic integro-differential equations regarding stochastic Brownian motion. Results in Applied Mathematics 2024; 24:100504. DOI: 10.1016/j.rinam.2024.100504

25. Badawi H, Abu Arqub OA, and Shawagfeh N. Existence, uniqueness, and numerical analysis of fractional M-derivative stochastic integrodifferential models within the shifted Legendre–Gauss pseudospectral algorithm. Fluctuation and Noise Letters 2025; 24. DOI: 10.1142/S0219477525500555